An atomistic investigation on the mechanism of machining nanostructures when using single tip and multi-tip diamond tools

Zhen Tong[1,2,3], Yingchun Liang[3] , Xiangqian Jiang[2], Xichun Luo[1*,2]

1 Department of Design, Manufacture & Engineering Management, University of Strathclyde, Glasgow, G1 1XQ, UK

2 Centre for Precision Technologies, University of Huddersfield, Huddersfield, HD1 3DH, UK

3 Center for Precision Engineering, Harbin Institute of Technology, Harbin, 150001, China

[*]Email: xichun.luo@strath.ac.uk

Abstract

In our previous work, a scale-up fabrication approach to cost effectively manufacturing nano-gratings over large area has been developed through diamond turning by using a multi-tip diamond tool fabricated by Focused Ion Beam. The objective of this study is to gain an in-depth understanding of the mechanism of machining nanostructures on single crystal copper through diamond turning when using a single tip and a multi-tip nanoscale diamond tool. For this purpose atomistic models of a single tip tool for multi-pass cutting and a multi-tip tool for single-pass cutting were built, respectively. The nature of the cutting chip formation, dislocation nucleation and propagation, cutting forces, and temperature distribution during nanometric cutting processes were studied through molecular dynamics (MD) simulations. Results show that nanostructure generation process at steady cutting stage was governed by a strong localization of the dislocation movement and the dynamic equilibrium of chip-tool contact area. Except the apparent improvement of machining efficiency that proportional to the tool tip numbers, the nano-grooves generated by multi-tip tool also have higher centre symmetry than those machined by single tip tool. While the average tangential cutting force per tip were calculated all around 33.3 nN, a larger normal cutting force per tip being 54.1nN was observed when using a multi-tip tool. A concept of atomistic equivalent temperature was proposed and used to analysis the important features of temperature distribution during the machining process. The advantage, disadvantage and applicability of diamond turning using multi-tip tool were discussed in comparison with those of using single-tip tool. The findings suggest that diamond turning using multi-tip tool might be more applicable than using single tip tool when apply to scale-up fabrication of periodic nanostructures.

(Some figures in this article are in color only in the electronic version)

Keywords: molecular dynamics; nanometric cutting; multi-tip tool; nanostructure; machining mechanism

1. Introduction

In recent years, the design and fabrication of periodic nano-structured surface have drawn great interest in diverse research fields including optics and electronics, solar energy, cell biology, bioengineering and medical science [1-3]. Numerous nanofabrication technologies including optical and electron beam lithography, focused ion beam (FIB) milling, nano-imprinting, femtosecond laser machining have been developed up to date to produce small quantities of nano-structured device/materials. However, these methods do have their own limitations such as high operational costs due to the need of clean room operation, low efficiency, or requiring complex multi-step for production, or not capable of the fabrication of 3D nanostructures. Lack of new cost effective scale-up manufacturing approach has become a significant barrier to industry, especially SME's realizing 3D ultra precision nanostructures (nanometer level tolerance) for many applications.

Diamond turning using multi-tip single crystal diamond tools is a new promising approach to the fabrication of micro/nano structures [2, 4, 5]. The technical feasibility of diamond turning using multi-tip tools (with tool tip dimensions ranging from 15μm to 100μm) has been successfully demonstrated by researchers through ultra-precision turning/scratching operations for the fabrication of periodic micro groves [6], arrays [7], and diffraction gratings [5]. Recently, new progress was made by Sun et al. by whom nanoscale multi-tip diamond tools with pitch at 100 nm have been successfully fabricated by focused ion beam [2]. Through ultra-precision diamond turning operation, nano-gratings were successfully generated on nickel sample without observing tool wear after hundreds of meters cutting distance [2].

However, lack of support from systematic theoretical study has seriously hindered the advance and industrialization of this technique. The machining mechanisms of nanostructures when using multi-tip tool has not been fully understood up to date. As the tools and the machined structures are in a range of sub-microns or even nanometers, the influence of surface effects such as material side flow and elastic recovery on the integrity of machined nanostructures cannot be ignored. In addition, some critical questions are also needed to be addressed including the evaluation of the advantage, disadvantage and applicability of this novel technology. However, we cannot get quick answers through experiment work due to the limitations of the current real-time detect equipment. On the other hand, molecular dynamics (MD) simulation provides a solution for this problem which will be further reviewed in next section.

Undoubtedly, the theoretic results obtained through simulations will provide valuable feedback and guidance for further development of this new technique.

2. The state-of-the-art MD simulation study on nanometric cutting

MD simulation studies, in general, were initiated in the late 1950s by Alder and Wainwright in the field of statistical mechanics [8]. Since 1980s, the feasibility of using MD simulation method to study nanometric cutting processes has been demonstrated by many researchers [3, 9-15]. In the following part, only classical models and results pertaining to the studies of nanometric cutting of copper are selected and briefly reviewed.

Since 2000's MD simulations studies on nano-scratching of copper by a pin diamond tool have been reported by Fang (2000), Kim (2005) and Yan (2006, 2008) etc. Fang and his co-workers [9] have indentified the frictional coefficient and forces as a function of the pin angle. Kim et al. [10] reported that in the nano-indentation and scratching process, the nucleation of the dislocation plays more important role in determining the abrupt drop during stick-slip than subsequent propagation of partial dislocations. Yan et al. [11] have simulated the multiple scratching processes of using an atomic force microscope (AFM) tip and investigated the effect of the feed rate on the deformation of the machined surface. A deformation criterion relating the single-atom potential energy variation to atom lattice deformation was further explored and the simulation results showed that four states exist between AFM pin tool and the workpiece surface [12]. Moreover, MD models were also built successfully to investigate the role of friction and tool wear in nanometric machining of copper, such as the work done by Ye et al. [3], Maekawa et al. [13], Lin and Huang [8] etc. Recently, large scale MD model with model size up to 10 million atoms has been performed by Pei et al. [14] to study the “size effect” existed in nanometric cutting of copper. Using this model, they further quantified the effect of processing parameters on cutting force and lattice defects [15]. These studies have made significant contributions towards our understanding of the mechanics of nanometric cutting of copper. However, until now no experimental work or simulation model has been found to investigate the cutting process and the machining mechanism for nanostructures by using multi-tip diamond tools.

Therefore, the main purpose of the present paper is to carry out MD simulations to study the nanometric cutting process and to reveal the mechanism of machining nanostructures using multi-tip nanoscale

diamond tool. In order to benchmark the advantage and disadvantage of diamond turning using multi-tip nanoscale tools, a comparison between using single tip and multi-tip nanoscale tools in nanometrc cutting has been made from the aspects of cutting forces and temperature distribution during the machining process. Of course, the simulation may have their own limitations including the need to run at very high cutting speeds, but this may not be a serious limitation as long as we are interested in the general nature of the process without consideration of the speed effects.

3. MD simulation

3.1 Geometric model for MD simulation

To avoid the size effect induced by using period boundary condition [14], two large scale nanometric cutting models with free boundary condition in all directions were built, respectively (as shown in figure 1(b), (c)). The geometry of the cutting tools is shown in figure 1 (a). The tool-tip width is 15a (a = 3.567 Å) with the tool rake angle α being 0º and the tool clearance angle β being 12º. To save the computational time, a double-tip nanoscale diamond tool with a pitch of 10a is employed in this paper to represent the multi-tip nanoscale tool. Both of the single tip and multi-tip nanoscale diamond tool are created based on perfect diamond crystal structure. Unlike previous research, where the diamond tool is treated as a rigid body, the tools built here are deformable body so as to track the cutting force and temperature distribution in the tool. Since the radius of cutting edge of diamond tool is usually larger than the minimum depth of cut in nanometric cutting, in our large-scale MD simulations, all of the tools are built with round cutting edge with an edge radius of 5a instead of a sharp cutting tool.

The workpiece has a dimension of $50a_0 \times 80a_0 \times 40a_0$ (a_0 = 3.615 Å) and consists of boundary layer and thermostat layer with thicknesses of $2a_0$ and $3a_0$, respectively (as shown in figure 1 (b) and (c)). Copper is chosen as workpiece material because of its high machinability when using diamond turning, particularly suitable for the fabrication of master tools used in roll-to-roll manufacturing [6]. The three orientations of the workpiece are [1 0 0], [0 1 0] and [0 0 1] in the X, Y and Z directions.

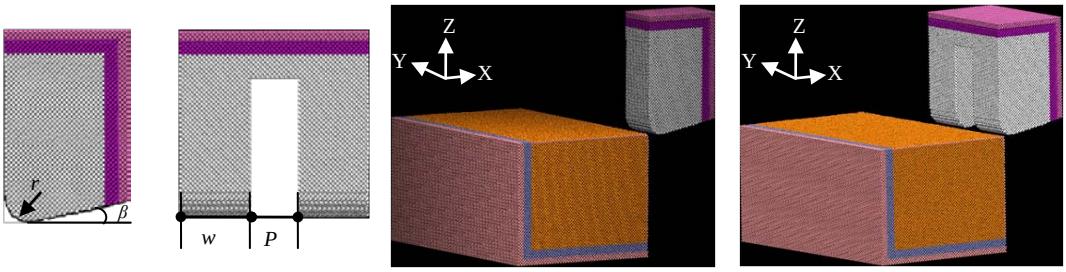

(a) Tool geometry (b) Single tip model (c) Multi-tip tool model

Figure 1. Models of MD cutting simulation

3.2 Potential functions for MD Simulation

There are three different atomic interactions in the MD simulation: (1) the interaction between copper atoms (Cu–Cu) in the workpiece; (2) the interaction between diamond atoms (C–C) in the tool; (3) the interaction between workpiece and tool (Cu–C). For the Cu–Cu interaction the embedded atom method (EAM) potential proposed by Foiles et al. [17] is used since it has been widely used in description of metal materials [3, 14, 20]. As it is shown in the Eq. (1), the total energy E of the atomistic system comprises summation over the atomistic aggregate of the individual embedding energy F_i of atom i and pair potential ϕ_{ij} between atom i and its neighboring atom j,

$$E = \sum_i F^i\left(\sum_{j\neq i}^{n} \rho^i\left(r^{ij}\right)\right) + \frac{1}{2}\sum_{ij,i\neq j} \phi_{ij}\left(r^{ij}\right) \tag{1}$$

where the lower case Latin superscripts i and j refer to atoms, r^{ij} is the distance between atoms i and j, and ρ^i is the electron density of atom i.

For C-C atoms, we adopt Tersoff potential [18] and computed as follows:

$$V_{ij} = f_C(r_{ij})\left[f_R(r_{ij}) + b_{ij} f_A(r_{ij})\right] \tag{2}$$

$$f_C(r) = \begin{cases} 1 : & r < R - D \\ \frac{1}{2} - \frac{1}{2}\sin\left(\frac{\pi}{2}\frac{r-R}{D}\right) : & R - D < r < R + D \\ 0 : & r > R + D \end{cases} \tag{3}$$

$$f_R(r) = Aexp(-\lambda_1 r) \qquad f_A(r) = -Bexp(-\lambda_2 r) \tag{4}$$

$$b_{ij} = \left(1 + \beta^n {\zeta_{ij}}^n\right)^{-\frac{1}{2n}} \qquad \zeta_{ij} = \sum_{k\neq i,j} f_C(r_{ik}) g\left(\theta_{ijk}\right) exp\left[{\lambda_3}^3 \left(r_{ij} - r_{ik}\right)^m\right] \tag{5}$$

$$g\left(\theta_{ijk}\right) = \gamma_{ijk}\left(1 + \frac{c^2}{d^2} - \frac{c^2}{[d^2 + (\cos\theta - \cos\theta_0)^2]}\right) \tag{6}$$

where V_{ij} is the bond energy about all the atomic bonds, i, j, k label the atoms of the system, r_{ij} is the length of the ij bond, b_{ij} is the bond order term, θ_{ijk} is the bond angle between the bonds ij and ik, f_R is a two-body term and f_A includes three-body interactions. f_C merely represents a smooth cutoff function to limit the

range of the potential, and ζ_{ij} counts the number of other bonds to atom *i* besides the *ij* bond.

Morse potential function is selected to descript the interaction between Cu-C, which has been widely used in MD simulations of nanometric cutting of Cu [11, 12]. The parameters are: D = 0.087eV, α = 5.14 Å^{-1}, r_0 = 2.05 Å.

3.3 MD simulation setup

All of the cutting tools are applied along the [-1 0 0] direction on the (0 0 1) surface of the copper at a constant cutting speed of 200m/s. The main computational parameters used in the MD simulations are summarized in table 1 for reference.

Table 1. Simulation parameters

	Single tip with multi-pass	Multi-tip with single pass
Workpiece material	Copper	Copper
Workpiece dimension	$50a_0 \times 80a_0 \times 40a_0$ (a_0 = 3.615 Å)	$50a_0 \times 80a_0 \times 40a_0$ (a_0 = 3.615 Å)
Number of atoms	760, 355	894, 870
Tool tip width	15a (a = 3.567 Å)	15a (a = 3.567 Å)
Tool rake angle	0º	0º
Tool clearance angle	12º	12º
Time step	1 fs	1 fs
Initial temperature	293K	293K
Depth of cut	1nm	1nm
Cutting speed	200m/s	200m/s

The equations of atoms motion were integrated using velocity-verlet algorithm with a time step of 1 fs. Moreover, 85,000 time steps were carried out as the relaxation process for fully free relaxation of the system to 293 K before cutting. During cutting the temperature was controlled by rescaling the thermal atoms velocities to 293 K if the temperature departs more than 5 K from the specified temperature at certain time step. This algorithm allows the heat transferring from shear region to the bulk of the workpiece which conform to experimental observation. All simulations were run with the system controlled by NVE ensemble.

Figure 2 shows the simulation procedure of nanometric cutting and traces of the tool. For single tip tool, it scratched the surface in X-Y plane along the OC direction for the first cutting pass (as shown in figure 2 (a)). Then the tool followed trace (C–C1) in the Y–Z plane. The tool moved along line C1A1 and moved down to point A. At last, the tool scratched the second groove along the line AB with same depth of cut (as the dotted line shown). For multi-tip tool, only single pass was taken with the same cutting distance as shown in figure 2 (b).

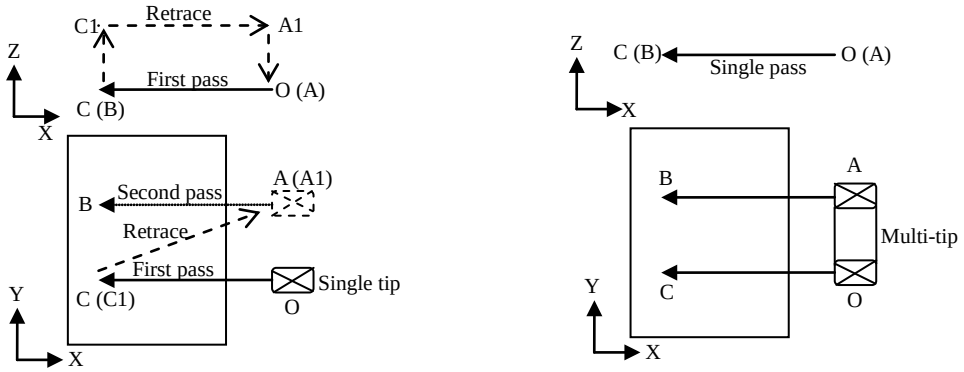

(a) Single tip cutting with two passes (b) Multi-tip cutting with single pass

Figure 2. Schematic of MD cutting traces

MD simulation was implemented by using an open source code — LAMMPS [16]. Some algorithms self-programmed for analysis of data will be introduced in the later section. All of the simulations were performed by high performance computing cluster (HPC) using 24 cores.

3.4 The visualization of atomistic configurations

The visualization of the variation of atomistic configurations during the cutting process was realized by VMD (Visual Molecular Dynamics) software. It has been found that centro-symmetry parameter (CSP) is less sensitive to the temperature increase compared with other methods such as atomic coordinate number and the slip vector [14]. The centro-symmetry parameter P_i for each atom is defined as follows,

$$P_i = \sum_{i=1}^{6} |\boldsymbol{R_i} + \boldsymbol{R_{i+6}}|^2 \tag{7}$$

where $\boldsymbol{R_i}$ and $\boldsymbol{R_{i+6}}$ are the vectors corresponding to the six pairs of opposite nearest atoms. The parameter P increases from 0 for perfect FCC lattice to positive values for defects and for atoms close to free surfaces. In the case of single crystal copper, the default value of P_i corresponding to those atomic defect structures and its represent color are indicated in table 2. (This color scheme can be seen on the web version of the article)

Table 2. The default value of atomic defects structure in CSP

Lattice Structure	Pi	Represent Atoms Color
Ideal FCC structure	P < 3	Yellow
Partial dislocation	3 < P < 5	Cyan
Stacking fault	5 < P < 8	Blue
Surface atoms	8< P <21.5	Orange
Surface edge atoms	P> 21.5	Pink

4. Results and discussions

4.1 Formation of Nanostructures

We first simulated the generation process of nanostructures on the (001) surface using the single tip tool

with two passes. It should be noted that the distance between two passes are specified with 10*a* (*a* = 3.567 Å) according to the pitch of the multi-tip tool. Figure 3 shows the snapshots of nanometric cutting process as well as the atomistic dislocation evolutions in the workpiece using single tip tool with a depth of cut of 1.0 nm. Each workpiece atom was colored by CSP value. It should be pointed out that the isolated atoms with green color which are inside the workpiece are not lattice defects. Those atoms with CSP above three are caused by the thermal vibration at finite temperature [14, 19]. Moreover, the defect-free atoms were removed from the visualizations.

For single tip tool cutting, it was found that at initial cutting stage, with the penetration of the tool cutting edge, the lattice of workpiece atom was deformed as buckled, and the outer kinetic energy of tool transmitted onto the workpiece and converted into potential energy stored in the deformed lattice. When this energy or shear stress of atoms exceeds a specific level, the atoms tend to re-arranged into lower energy lattice to relax lattice strain through dislocation nucleation (as shown in figure 3 (a)). With increase of cutting distance, more and more dislocations initiated and propagated in preferred (111) crystal slip planes systems, and some atoms accumulated and piled up in front of the tool rake face leading to the formation of cutting chip (as shown in figure 3 (b)). These results agreed well with former researcher's analysis on the evolution of dislocation nucleation and propagation process during the nanometric cutting process of copper.

Second pass was taken along line AB with same processing parameters (as shown in figure 2 (a)). After two concessive cutting passes, two nano-grooves were machined by single tip tool (as shown in figure 3 (c)). Fang [20] and Yan et al. [11] have reported that when the distance between the first and second scratch was larger than the tip radius (for pin shape tool), the state of first scratch was very close to that of the second one. Our results agree with their conclusions and fulfilled it by further confirmed that this phenomenon happens not only in pin shape tool but also in rectangle shape tool-tip. In our simulation model, the distance between two passes are specified with 10*a* (*a* = 3.567 Å) according to the tip-pitch of the multi-tip tool. As shown in figure 3 (c), the shape of two nano-grooves formed are nearly the same, which will be further confirmed by the similarly cutting force discussed in next section (as shown in figure 6). However, it should be noted that at the end of the second pass, there were some disordered atoms moved into the first nano-groove and result in re-shaping the right side of the first groove. This

indicated that material side flow appeared in the nanometric cutting when using single-tip tool due to the formation and movements of dislocations. When the distance between two passes is less than a critical value, there is a strong possibility that the dislocation generated by second pass will extend and affect the finished surface of the first cutting pass, thus resulting in represent of first nano-groove. However, it is noted that this critical value is not fixed as the dislocation nucleation and movements are affected by the tool geometry, depth of cut, cutting speed and local temperature [19].

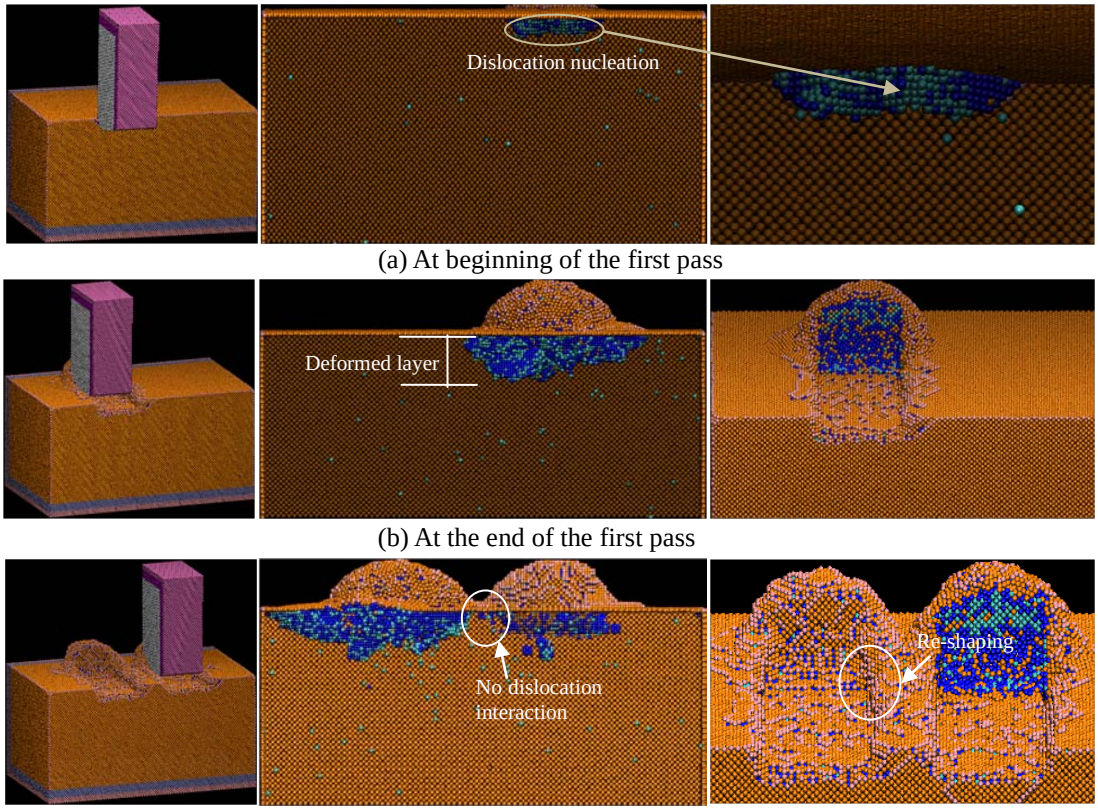

(a) At beginning of the first pass

(b) At the end of the first pass

(c) At the end of the second pass

Figure 3. Snapshots of cutting process and dislocation evolution of workpiece using a single tip tool with multi-tip passes.

For multi-tip tool cutting, it can be seen from figure 4 (a) and (b) that the initial cutting stage was almost the same as that of using single tip tool, i.e. dislocations initiated under the tool-workpiece contact region due to the compressive stress induced by initial impact of the tool tips, and then propagated along the (111) crystal slip planes systems. The atoms further accumulated and piled up result in the formation of two independent initial chips. However, unlike single tip cutting, where the nano-grooves were formed one by one through two passes separately, significant interactions between dislocations around tool tips were observed when using multi-tip tool (as shown by figure 4 (b)), which resulted in dislocation pile-up in Z direction and leading to a larger normal cutting force (as shown by figure 6). Moreover, owing to the

special tool geometry offered by multi-tip tool, the multi-tip tool was able to overcome the effect of side flow and generated two nano-grooves through single pass with higher centre symmetry (as shown in figure 4 (c)). However, this does not mean that the multi-tip tool has absolute advantage than the single tip tool to form nanostructures. The structures generation processes are accompanied by the fluctuation of cutting forces and generation of cutting heat, which will influence the formation of nanostructures. They will be further discussed in the following sections.

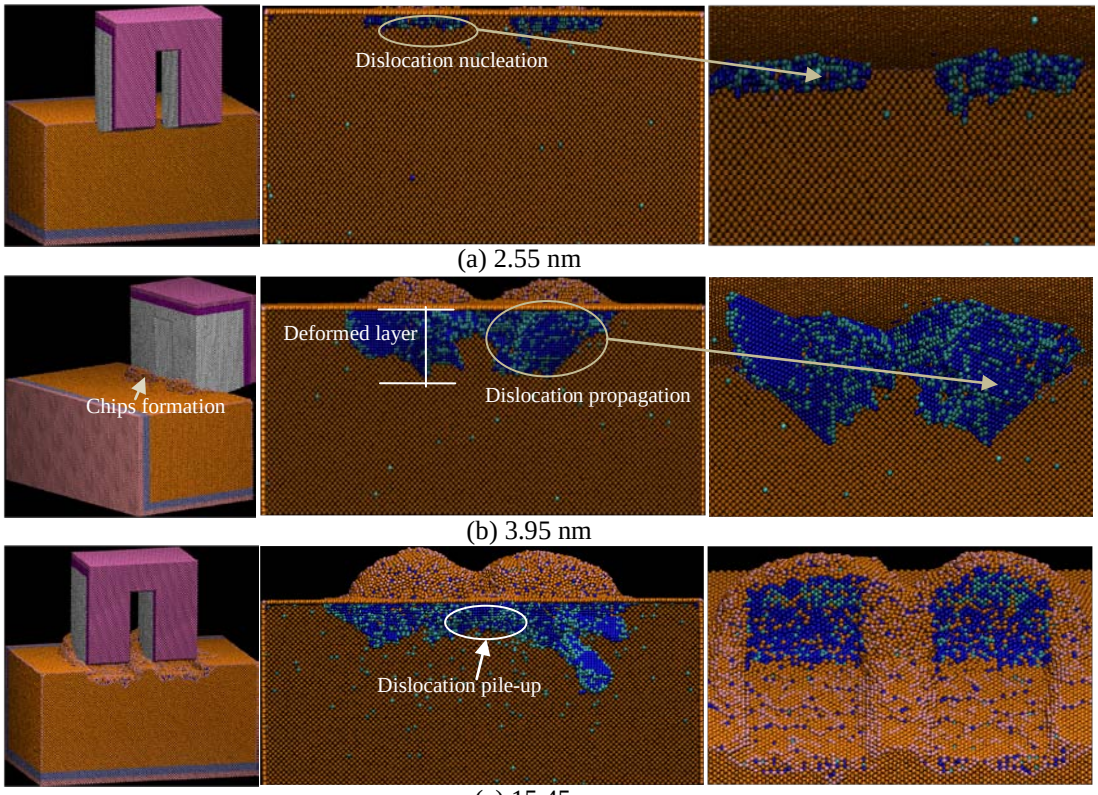

Figure 4. Snapshots of cutting process and dislocation evolution of workpiece using a multi-tip tool.

4.2 Cutting force and friction

The cutting forces were obtained by summing the forces of tool atoms. A schematic diagram of these forces directions was shown in figure 5 (a). The variation of cutting force in the X, Y, and Z directions during the steady cutting process were summarized in figure 5 (b). It is noted that the comparison was made between the first and the second pass of single tip and multi-tip. It can been found that the tangential cutting force F_x and normal cutting force F_z of all simulations are fluctuated around a constant value at the steady cutting stage. Correlating with the snapshot of dislocation evolution shown in figure 2 and figure 3, these simulations results indicate that the cutting forces tend to be in a steady state after the

initial formation of chips. Although the tool-workpiece contact area increased while the workpiece atoms piled up in front of the tool rake face to form chips, the contact area reached dynamic equilibrium at the steady cutting stage. Meanwhile, the outer mechanical energy of the tool partly converted into thermal energy in terms of cutting heat which was generated from the friction behavior between the tool cutting edge and the workpiece. However, the cutting forces in the Y direction for all simulations were found to have an average value near zero during the cutting process because of the balanced forces contributing from each side.

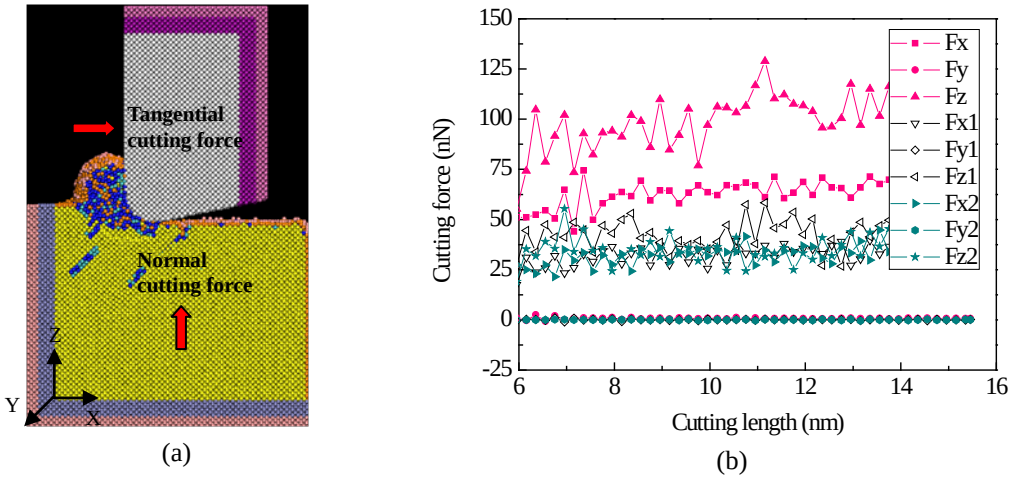

Figure 5. Cutting force during nanometric cutting process. (a) Direction of cutting forces. (b) The force-displacement curves at the depth of cut of 1nm. F_x, F_y and F_z represent the cutting forces of using multi-tip tools; F_{x1}, F_{y1}, F_{z1} and F_{x2}, F_{y2} and F_{z2} represent the forces for 1st and 2nd pass using single tip tools, respectively.

In order to further quantify the difference of cutting force during nanostructure formation process, the average tangential cutting forces and normal cutting forces at the steady cutting state were calculated (as shown in figure 6). It was found that the tangential cutting force of the first and second cutting pass when using single tip tool were nearly the same, but the normal cutting force of second pass was smaller than that of the first pass. This phenomenon is caused by the side flow appeared at the end of second pass (as shown in figure 3 (c)). The movement of dislocations was accompanied by the plastic side flow which released the extra stress during second pass and thus resulted in a smaller normal cutting force in comparison with the first pass. However, for multi-tip tool cutting, while the tangential cutting force per tip of multi-tip tool has a value of 33.3nN which is slightly smaller than that of using a single tip tool; the value of normal cutting force per tip being 54.1nN is much larger than those of using the single tip tool (46.9nN for the first pass, 38.5nN for the second pass). The dislocation evolution discussed above indicated that there was a local strengthen of the material in normal direction during multi-tip cutting

process which was mainly due to the significant dislocation pile-up beneath the tool tips.

The ratio of tangential cutting force to normal cutting force which indicates the coefficient of friction ($\mu=F_x/F_z$) is used to assess the alternation of local physical property during the nanometric cutting process. From the average forces at the steady stage, we obtain $\mu \approx 0.61$ for multi-tip cutting and a slightly larger average value of 0.82 for single tip tool. Our calculated value of μ agrees with the experimentally results measured by Lin et al. They reported that in scratching copper the actual tangential cutting force F_x being 2780.2 nN and normal cutting force F_z being 5686.2 nN [8]. Here we generated coefficient of friction from their experiment data and it is 0.49. It is not surprising that our calculated coefficients of friction is little larger than experimental result as the coefficient of friction also depends on the surface smoothness and crystal structure of materials used.

In nature, Luan and Robbins have argued that the atomic-scale surface roughness produced by discrete atoms had significant effect on coefficient of friction, and the contact areas and stresses may be changed with the local alternation of friction and lateral contact stiffness in an order of magnitude [21]. This finding explained the fluctuation of cutting forces and the difference of frictional coefficient observed in present simulations when using the single tip tool and multi-tip tool. For multi-tip tool cutting, the friction between the tool and workpiece was smaller than that of using single tip tool because of the difference of local tool-workpiece contact status and thermal soften effect which will be further discussed in the following section.

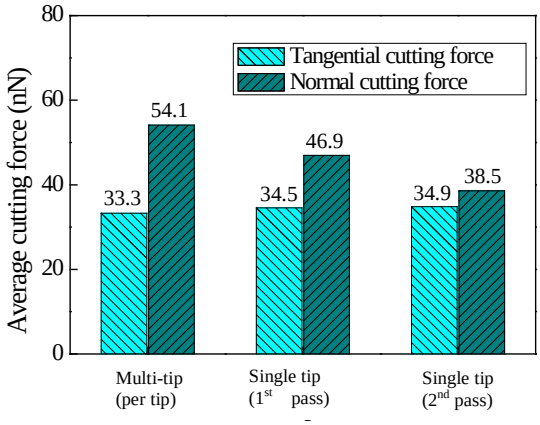

Figure 6. The average cutting forces of the single tip and multi-tip tools cutting.

4.3 Temperature distribution

It is well known that the translation between kinetic energy and temperature can be calculated using the law of equipartition of energy. However, the kinetic energy of single atom could not be directly

transformed into temperature as the nature of the temperature is statistical. In order to reveal the temperature distribution during the nanometric cutting process, we proposed a concept of atomistic equivalent temperature T_i which is calculated from the statistical average temperature of neighbour atoms around atom *i*. A critical radius $r_0$was employed to select the neighbour atoms, and the translation between atoms kinetic energy and statistical temperature were computed using the equation bellow:

$$\frac{1}{2}\sum_{j=1}^{n} m_j v_j^2 = \frac{3}{2} n k_B T_i \tag{8}$$

where n is the number of atoms within radius r_0, m_j and v_j represent the mass and instantaneous velocity respectively, $k_B$is the Boltzmann constant.

Figure 7 shows the cross-sectional view of the temperature distribution during the nanometric cutting process for using single tip tool and multi-tip tool, respectively. Various temperature zones with different colors were used to distinguish the system temperature distribution during the cutting process. It can be seen that in all of the simulations, the temperature in shear zone was about 650K, and the highest temperature was found in the chip (about 900K). However, in comparison with the high temperature distributed at workpiece, a relative lower temperature (around 550 K) was found in tool cutting edge attributed to the high thermal conductivity of diamond materials, which provide significant theoretical support to the feasibility of using nanoscale diamond tools to generate nanostructures. Nevertheless, it should be pointed out that the range of high temperature region (>500K) of using multi-tip tool was apparently larger than that of using single tip tool (as shown in figure 7 (c)). This important phenomenon well explained the difference of cutting force and the frictional coefficient discussed in the above section. Although the chip volume and the normal cutting force per tip of the multi-tip cutting were larger than that of using the single tip tool, the tangential cutting force per tip is slightly lower than that of using the single tip tool (as shown in figure 6). It indicates that the higher local temperature generated during the multi-tip cutting process would result in local weakening of the Cu-Cu bond force, and thus leading to a lower tangential cutting force per tip.

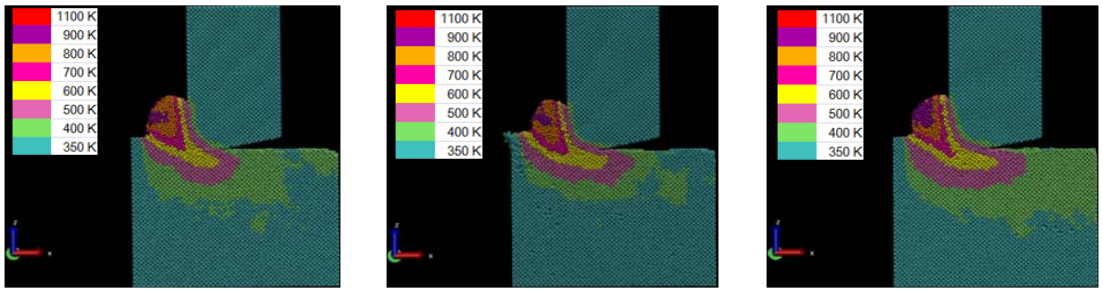

(a) Single tip first pass (b) Single tip second pass (c) Multi-tip

Figure 7. The cross-section view of temperature distribution at depth of cut of 1 nm.

Currently, the minimum line width that can be obtained through single point diamond turning (SPDT) is significantly limited by the dimension of the cutting tools. By applying the advanced FIB milling technique, it is possible to generate micro/nano structures on diamond tool tip to obtain various kinds of multi-tip nanoscale diamond tools. In addition, except the high efficiency which is proportional to the number of tool tip used, the nanostructure generated by the multi-tip tool also has better central symmetry than the one machined by using the single tip tool owing to the special geometry design of the multi-tip tool. Therefore, diamond turning using nanoscale multi-tip tool is a promising technique for massive fabrication of nanostructure—a new technique that needs to be further explored and developed.

5. Conclusions

In this work, large-scale MD simulations have been performed to study the naometric cutting process when using single tip tools and multi-tip tools. Based on the simulation results, conclusions are drawn as follows:

(1) The formation mechanism of nanostructures by using single tip tools and multi-tip tools are different. The nanostructure generation process at steady cutting stage was governed by strong localization of the dislocation movement and dynamic equilibrium of the chip-tool contact area. Side flow appeared when using single tip tool. While no side flow effect was observed when using multi-tip tool and the nanostructure generated by the multi-tip tool have better central symmetry than those machined by the single tip tool. This feature make multi-tip tool cutting more practicable and applicable for scale-up fabrication of periodic nanostructures.

(2) In all simulations the cutting forces at steady cutting stage fluctuated around a constant value after chip formation. The value of the average normal cutting force per tip of using the multi-tip tool was much larger than that of using the single tip tool. The significant dislocation pile-up beneath the tips of multi-tip

tool resulted in local strengthens of the material in the normal direction.

(3) Under the nanometric cutting condition used in the present work, the frictional coefficient between the tool and the workpiece by using the multi-tip tool is smaller than that of using the single tip tool. This alternation was resulted from the difference of local tool-workpiece contact status and the thermal soften effect during nanostructure generation process.

(4) The proposed algorithm of atomistic equivalent temperature was suitable for the identification of local temperature distribution during the nanometric cutting process. In comparison with the high temperature region distributing in chips, relative low local temperature distributed at the tool cutting edge provided important theoretical support of using multi-tip nanoscale diamond tools for the fabrication of nanostructures.

Acknowledgment

The authors gratefully acknowledge the financial support from EPSRC (EP/K018345/1), Sino-UK Higher Education Research Partnership for PhD Studies (CPT508) and the National Funds for Distinguished Young Scholars (No.50925521) of China. The authors would also like to acknowledge the technical supports from the HPC team at the University of Huddersfield and assess to Huddersfield Queensgate Grid for MD simulations in this study.

References

[1] L.B. Kong, D.F. Cheung, X.Q. Jiang, W.B. Lee, S. To, L. Blunt, P. Scott, Precis. Eng. **34** (2010) 75–766.

[2] J. Sun, X. Luo, W. Chang, M.J. Ritchie, J. Chien, A. Lee, J. Micromech. Microeng. **22** (2012) 115014.

[3] Y.Y. Ye, R. Biswas, J.R. Morris, A. Bastawros, A. Chandra, Nanotechnology **14** (2003) 390–396.

[4] D.P. Adamsa, M.J. Vasile, A.S.M. Krishnan, Precis. Eng. **24** (2000) 347–356.

[5] Z.W. Xu, F.Z. Fang, S.J. Zhang, X.D. Zhang, X.T. Hu, Y.Q. Fu, L. Li, Opt. Expr. **18** (8) (2010) 8025–8032.

[6] Y.N. Picard, D.P. Adams, M.J. Vasile, M.B. Ritchey, Precis. Eng. **27** (1) (2003) 59–69.

[7] X. Ding, G.C. Lim, C.K. Cheng, D.B. Lee, K.C. Shaw, K. Liu, W.S. Fong, J. Micromech. Microeng. **18** (2008) 075017.

[8] Z.C. Lin, J.C. Huang, Nanotechnology **19** (2008) 115701.

[9] T.H. Fang, C.I. Weng, Nanotechnology **11** (2000) 148–153.

[10] M.H. Cho, S.J. Kim, D.S. Lim, H. Jang, Wear **259** (7–12) (2005) 1392–1399.

[11] Y.D. Yan, T. Sun, S. Dong, C. Liang, Comput. Mater. Sci. **40** (1) (2007) 1–5.

[12] Y.D. Yan, T. Sun, S. Dong, X.C. Luo, Y.C. Liang, Appl. Surf. Sci. **252** (20) (2006) 7523–7531.

[13] K. Maekawa, A. Itoh, Wear **188** (1–2) (1995) 115–122.

[14] Q.X. Pei, C. Lu, H.P. Lee, Y.W. Zhang, Nanoscale Res. Lett. **4** (2009) 444–451.

[15] Q.X. Pei, C. Lu, H.P. Lee, Comput. Mater. Sci. **41** (2) (2007) 177–185.

[16] S.J. Plimpton, J. Comput. Phys. **117** (1995) 1–19.

[17] S.M. Foiles, M.I. Baskes, M.S. Daw, Phys. Rev. B **33** (1986) 7983–7991.

[18] J. Tersoff, Phys Rev B, Condens. Matter. **37** (12) (1988) 6991–7000.

[19] P.Z. Zhu, Y.Z. Hu, T.B. Ma, H. Wang, Appl. Surf. Sci. **256** (23) (2010) 7160–7165.

[20] T.H. Fang, C.I. Weng, J.G. Chang, Surf. Sci. **501** (2002) 138–147.

[21] B. Luan, M.O. Robbins, Nature **435** (2005) 929–932.